

ARTICLES

The OH Product State Distribution from the Photodissociation of Hexafluoroacetylacetone

Min-Chul Yoon, Young S. Choi, and Sang Kyu Kim*

Department of Chemistry, Inha University, Incheon (402–751), Republic of Korea

Received: October 29, 1999; In Final Form: January 11, 2000

Hexafluoroacetylacetone (1,1,1,5,5,5-hexafluoro-2,4-pentanedione) in the supersonic jet, which exists as its enolic form, has been found to give the OH radical as a result of photodissociation induced by the $\pi-\pi^*$ transition. The nascent OH product state distributions are measured at the photolysis wavelengths of 293.5 and 266 nm. As in the case of the acetylacetone photodissociation, no fluorescence is observed even in the energy region near the origin, indicating ultrafast nonradiative decay of the excited state. The OH fragment is found to be vibrationally cold, and its rotational state distributions are peaked at $N = 3$ at both pump wavelengths used in this work. The OH fragment is slightly more populated in the ${}^2\Pi_{3/2}$ state than it is in the ${}^2\Pi_{1/2}$ state. The Π^-/Π^+ ratios are found to be unity, suggesting that there is no preferential alignment of the $p\pi$ electronic orbital of the OH radical with respect to its plane of rotation. The strength of the intramolecular hydrogen bond and its dynamic role in the chemical bond dissociation of hexafluoroacetylacetone are discussed and compared with the acetylacetone photodissociation dynamics.

I. Introduction

The β -diketone compounds are intriguing molecules because they have two different structural isomers: diketo and enol. The relative population of these two isomers varies depending on the characteristics of the environment.^{1,2} For instance, most β -diketone compounds exist predominantly as enol forms in the gas phase at room temperature.^{1,2} The preferential population of the enol form in the gas phase is known to be due to the formation of a relatively strong intramolecular hydrogen bond in the enolic β -diketones. The strengths of the intramolecular hydrogen bonds in the enolic β -diketones have not been experimentally measured. However, the stabilization energy of the hydrogen bond of the enolic acetylacetone has been theoretically predicted to be around 12 kcal/mol,³ which is much stronger than the usual intermolecular hydrogen-bond energy of 3–4 kcal/mol. Because of the strong intramolecular hydrogen bonding, the structure^{4–8} and proton-transfer dynamics^{9–12} of enolic β -diketones have been subjects of intensive theoretical and experimental studies for past decades.

The photochemistry of β -diketones, however, has not been given that much attention until quite recently. The acetylacetone molecule is the first one that has been investigated as a model compound for the photochemical study.^{13,14} According to UV² and electron-impact¹⁵ spectroscopic studies, the enolic acetylacetone in the gas phase has a broad structureless absorption band peaked at around 270 nm, which is attributed to the electronically allowed $\pi-\pi^*$ transition. Roubin et al.¹⁶ have shown that in the matrix environment, the acetylacetone molecule undergoes the stereoisomerization upon the UV irradiation. Recently, our group reported the first photochemical study of the gas-phase acetylacetone.^{13,14} Interestingly, the enolic acetylacetone has

been found to produce the OH fragment as a consequence of the chemical bond dissociation induced by the $\pi-\pi^*$ transition. The nature of the potential energy surface where the dissociation takes place and the role of the intramolecular hydrogen-bond in the bond-breaking event of acetylacetone were discussed in the previous works.^{13,14}

In this work, we investigate the photodissociation dynamics of hexafluoroacetylacetone. From IR¹⁷ and NMR¹⁸ spectroscopic studies, the intramolecular hydrogen-bonding of hexafluoroacetylacetone has been known to be weaker compared to that of acetylacetone. We have found here that hexafluoroacetylacetone also gives rise to the OH fragment upon the $\pi-\pi^*$ transition. From the analysis of the OH product state distribution, the effects of the H/F substitution of two methyl groups of acetylacetone on the intramolecular hydrogen-bond strength and the chemical bond dissociation dynamics are investigated.

II. Experimental Section

Experimental conditions were described elsewhere.¹⁴ Briefly, hexafluoroacetylacetone (Aldrich, 98%) was purchased and used without further purification. Hexafluoroacetylacetone was heated at 50 °C and the He carrier gas was passed through the sample. The gas mixture was then expanded through a nozzle orifice (General Valve, 0.5 mm diameter) into a vacuum chamber with a backing pressure of ~ 1 atm. The background pressure of the chamber was maintained at $\sim 10^{-5}$ Torr when the nozzle (10 Hz) was on. The nozzle was heated to 70 °C both to reduce cluster formation and sample condensation.

The second harmonic output of a Nd:YAG laser (Spectra-Physics, GCR-150, 10 Hz, 7 ns duration) was split in half to pump two independently tunable dye lasers. One dye laser (Lumonics, HD-500) was used to generate the laser pulses in the 585–600 nm region. The output of the dye laser was

* To whom correspondence should be addressed (E-mail: skkim@inha.ac.kr).

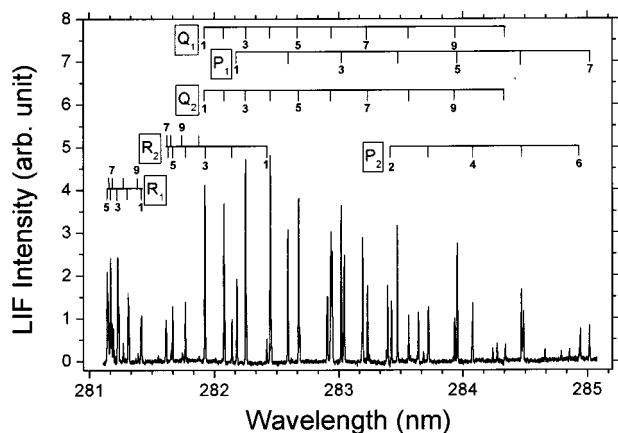


Figure 1. A typical OH LIF spectrum taken at $\lambda_{\text{pump}} = 266$ nm with appropriate assignments. The subscripts 1 and 2 represent the ${}^2\Pi_{3/2}$ and ${}^2\Pi_{1/2}$ states, respectively.

frequency-doubled via a KD*P crystal to generate the UV laser pulses in the 292.5–300 nm region to be used to excite the molecule (the pump laser pulse). The other dye laser (Lamda-Physik, Scanmate II) was used to generate the UV laser pulse in the 280–290 nm range after the frequency-doubling. This probe laser pulse was used to probe the nascent OH fragment from the hexafluoroacetylacetone dissociation. The second harmonic crystal was placed on a homemade crystal tracking system to maintain both the direction and intensity of the UV output. The fourth harmonic output (266 nm) of the Nd:YAG laser was also used for the pump.

The pump and probe laser pulses were combined with a dichroic mirror, directed into the vacuum chamber, and overlapped with a molecular beam located 20 mm downstream from the nozzle orifice. The delay time between the pump and probe laser pulses was fixed at 10 ns. The polarization of the pump laser was perpendicular to the direction of the fluorescence detection. The fluctuation of the probe laser intensity was monitored with a photodiode and used for the normalization of the signal. The laser-induced fluorescence (LIF) signal was detected through a photomultiplier tube (PMT) (Hamamatsu, H-1949–50), integrated by a boxcar (SRS, SR250), A/D converted by an interface (SRS, SR245), and stored in an IBM personal computer using a data-taking program which also controlled two dye lasers and crystal-tracking systems. The intensity of the probe laser was much reduced so that the OH transition would not be saturated. The linearity of the LIF signal with the probe laser intensity was carefully checked. The LIF signal was averaged for 10 laser shots and the LIF spectra were taken at least three times at each photolysis wavelength.

III. Results and Discussion

The $A^2\Sigma^+(v' = 1) - X^2\Pi(v'' = 0)$ transition of OH is used for the LIF measurement. A typical LIF spectrum of the OH fragment from the hexafluoroacetylacetone photodissociation at 266 nm is shown in Figure 1 with appropriate assignments for the observed peaks.¹⁹ The OH transitions are labeled according to Hund's case (b). The P, Q, and R branches represent the transitions for $\Delta N = -1, 0,$ and $1,$ respectively. The subscripts 1 and 2 are for the $\Pi_{3/2}$ and $\Pi_{1/2}$ states, respectively. The relative populations of the OH fragment are determined by dividing the LIF intensities by their corresponding Einstein absorption coefficients.²⁰

No fluorescence has been observed from the excited hexafluoroacetylacetone, which suggests the ultrafast decay of the excited

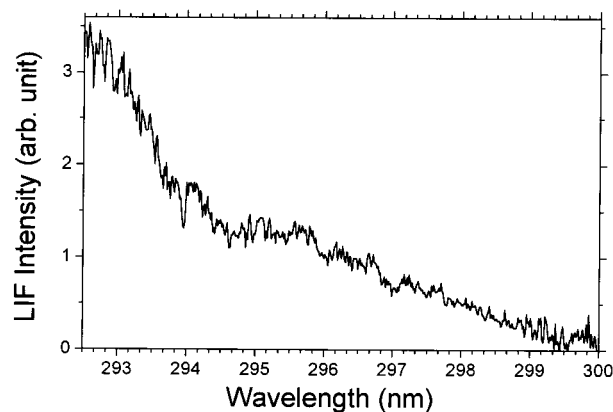


Figure 2. Photofragment excitation (PHOFEX) spectrum which monitors the OH LIF intensity due to the $P_1(4)$ transition as a continuous function of the pump wavelength. The delay time between pump and probe laser pulses is fixed at 10 ns.

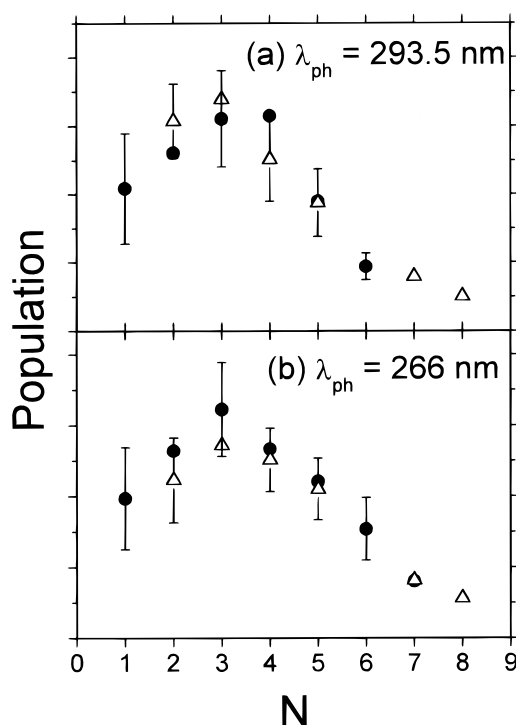


Figure 3. The OH rotational state distributions at (a) 293.5 and (b) 266 nm in the ${}^2\Pi_{3/2}$ state. The filled circles and open triangles represent distributions in the $\Pi^+(A')$ and $\Pi^-(A'')$ states, respectively.

state via nonradiative processes. Thus, it is probable that the dissociation occurs on the lower electronic states following fast internal conversion or intersystem crossing processes. The photofragment excitation (PHOFEX) spectrum is taken by monitoring the LIF intensity due to the $P_1(4)$ transition as a continuous function of the pump wavelength, Figure 2. No distinct structure is observed even in the energy region near the electronic origin of ~ 300 nm. This observation is also consistent with the ultrafast nonradiative decay of the excited state.

A. OH Rotational State Distribution. The OH rotational distributions at 293.5 and 266 nm are determined by the analysis of the P, Q, and R branches from the $\Pi_{3/2}$ state, Figure 3. Because the P and R branches probe the same Λ -doublet level (Π^+, A'), the populations obtained from P and R branches are averaged to give the OH rotational state distribution in the ${}^2\Pi_{3/2}(A')$ state. The OH rotational distributions in the ${}^2\Pi_{3/2}(A'')$ state are obtained by analyzing the Q branches. The rotational

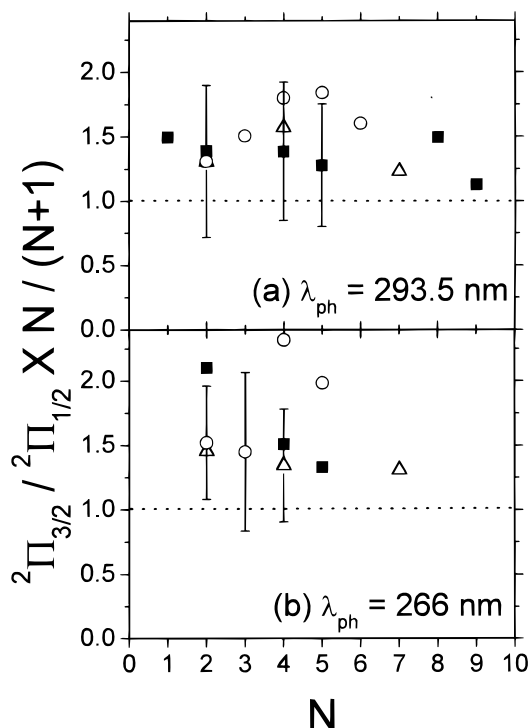


Figure 4. The spin-orbit ratios as a function of the rotational quantum number at (a) 293.5 and (b) 266 nm determined from the P_1/P_2 (open circles), Q_1/Q_2 (open triangles), and R_1/R_2 (filled rectangles) ratios. The ${}^2\Pi_{3/2}$ state is slightly more populated than the ${}^2\Pi_{1/2}$ state.

distributions at both pump wavelengths are peaked at $N = 3$. The OH fragment is found to be vibrationally cold; no LIF signal due to OH ($\nu'' = 1$) is detected with the present setup.

B. Spin-Orbit State Distributions. The spin-orbit ratios, multiplied by appropriate statistical weights, are found to be not unity when they are plotted versus the rotational quantum number, as shown in Figure 4. At both pump wavelengths, the ${}^2\Pi_{3/2}$ state is found to be slightly more populated compared to the ${}^2\Pi_{1/2}$ state. This OH spin preference has also been observed in the acetylacetone dissociation.¹⁴ The preferential population of the OH fragment in the ${}^2\Pi_{3/2}$ state has been observed for the acetic acid dissociation at 200 nm,²¹ and interpreted as being due to coupling of the initially excited singlet to a nearby triplet state. However, the origin of the nonstatistical population of the spin-orbit states for β -diketone compounds is not clear yet.

C. Population of the Λ -Doublets. The relative populations of the Λ -doublets of the OH fragment provide the information about the exit channel dynamics in the chemical bond breaking event. In the acetylacetone dissociation, it has been found that Λ -doublet states of the OH fragment are not statistically populated.¹⁴ According to the analysis in ref 14, the charge density of the $p\pi$ lobe of the OH fragment is found to be peaked at around 30° with respect to the plane of rotation, suggesting a small preference of the planar dissociation pathway of acetylacetone. Interestingly, however, the ${}^2\Pi_{3/2}(A'')/{}^2\Pi_{3/2}(A')$ ratios of the OH fragment from the hexafluoroacetylacetone dissociation are found to be unity at both 293.5 and 266 nm when they are plotted versus the OH rotational quantum number (N) in Figure 5. This indicates that the $p\pi$ lobe of the OH fragment is randomly oriented with respect to the rotating plane,²² which means a lack of strong dynamical constraint during the chemical-bond dissociation of hexafluoroacetylacetone.

The difference in the Λ -doublet ratios between acetylacetone and hexafluoroacetylacetone could originate from the difference

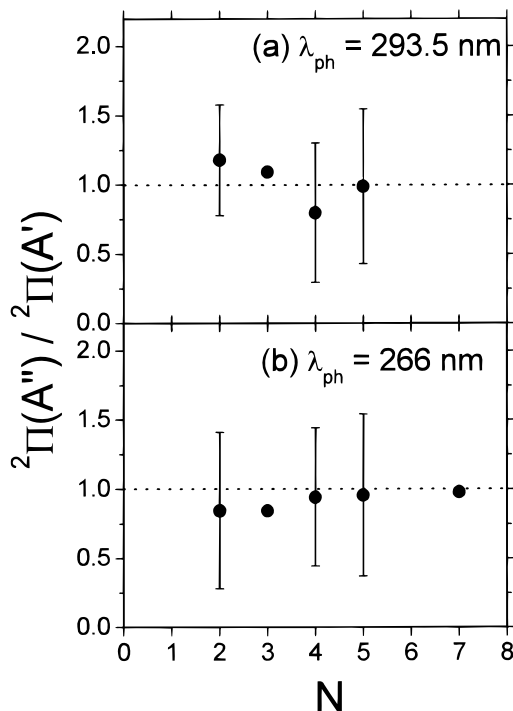


Figure 5. The Λ -doublet ratios versus $N(\text{OH})$ at (a) 293.5 and (b) 266 nm. The average values are close to unity.

in the intramolecular hydrogen-bond energies of two compounds, because it is the intramolecular hydrogen bond that maintains the planarity of the enolic β -diketones. As mentioned in the Introduction section, the enolic hexafluoroacetylacetone is known to form the weaker intramolecular hydrogen bond than does the enolic acetylacetone, because of the electron-withdrawing effect of two CF_3 groups of hexafluoroacetylacetone.^{17,18} Thus, it is possible that the relatively strong intramolecular hydrogen bond in acetylacetone plays a significant role in the chemical bond dissociation dynamics in terms of maintaining the molecular planarity to some extent, resulting in the non-statistical Λ -doublet ratio of the OH fragment.¹⁴ Meanwhile, the weaker intramolecular hydrogen bond in hexafluoroacetylacetone does not give the strong dynamical constraint during the chemical bond dissociation, giving the statistical population of the Λ -doublets.

D. Prior Calculation and the Intramolecular Hydrogen-Bond Strength. Prior calculation, which assumes that the product state distributions are determined by the number of energetically accessible quantum states of products, has been used for comparison with the experimental result for the acetylacetone photodissociation (see ref 14). The shape of the potential energy surface along the reaction coordinate for the dissociation of hexafluoroacetylacetone is not expected to be much different from that for the acetylacetone dissociation. Therefore, the prior calculation is also carried out here to be compared with the experiment for the hexafluoroacetylacetone dissociation.

Ab initio calculation with a 6-31+G(d) basis set on the Hartree-Fock level has been carried out for the ground state of the 1,1,1,5,5,5-hexafluoro-3-penten-2-on-4-yl radical using the GAUSSIAN 98 program.²³ The 33 normal-mode frequencies have been calculated. The relative population of OH (N) is determined by the number of energetically accessible quantum states of products at the energy, $E = E_{\text{avail}} - E_{\text{rot}}(\text{OH}, N)$. The rotational energy of the 1,1,1,5,5,5-hexafluoro-3-penten-2-on-4-yl radical is expected to be very small, and neglected in

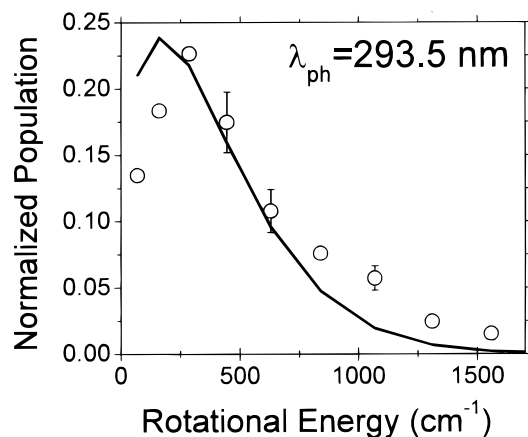


Figure 6. The experiment (open circles) at 293.5 nm and prior calculations when the C–O(H) bond dissociation energy is 90.3 kcal/mol (solid line).¹⁴

counting the number of states. Accordingly, the number of vibrational quantum states of the 1,1,1,5,5,5-hexafluoro-3-penten-2-on-4-yl radical, associated with the OH ($N, v'' = 0$), is counted using a Beyer–Swinehart algorithm,²⁴ and multiplied by the degeneracy factor of $(2J+1)$ to give the calculated distribution.

One of the most important factors in the prior calculation is the available energy for the products. However, it is nontrivial to estimate the energetics involved in the photodissociation process of hexafluoroacetylacetone. From ref 14, the upper bound for the C–O(H) bond dissociation energy of acetylacetone has been estimated to be 90.3 kcal/mol. Assuming the same C–O(H) bond dissociation energy for hexafluoroacetylacetone as that of acetylacetone, the prior calculation is carried out to give a solid line in Figure 6. The calculation matches the experiment very poorly; the prior calculation predicts the more population in the low N values and the less population in the high N values compared to the experiment.

The prior calculation was successful in reproducing the OH rotational state distribution from acetylacetone at 291 nm, whereas it failed to reproduce that at 266 nm.¹⁴ If the prior theory is assumed to be appropriate in explaining the OH rotational state distribution in the low-excess energy region above the reaction threshold, the mismatch between experiment and theory found in Figure 6 might require the modification of the excess energy in the prior calculation, indicating that less energy is needed to dissociate the C–O(H) bond of hexafluoroacetylacetone compared to that of acetylacetone. The weaker intramolecular hydrogen bond energy of hexafluoroacetylacetone than that of acetylacetone is also consistent with the statistical population of the Λ -doublets (vide supra). That is, contrary to the acetylacetone photodissociation case, because of the weaker hydrogen bond of the enolic hexafluoroacetylacetone, there is no strong dynamical constraint during the bond dissociation.

The reaction mechanism in the photodissociation of β -diketone compounds is not yet clearly resolved at this time. The measurement of the OH appearance rate as a function of the

pump energy would provide a good chance to test a variety of statistical theories for these interesting systems. In addition, the measurement of the OH translational energy distribution by Doppler analyses would also be very helpful to clarify the reaction mechanism further.

IV. Conclusions

Hexafluoroacetylacetone is found to give the OH fragment upon the π – π^* transition induced by UV irradiation. The nascent OH rotational state distributions measured at the pump wavelengths of 293.5 and 266 nm are determined by the laser-induced fluorescence technique. The ${}^2\Pi_{3/2}$ state is slightly more populated than the ${}^2\Pi_{1/2}$ state. The Λ -doublet states are found to be statistically populated, indicating that the $p\pi$ lobe of the OH fragment is randomly oriented with respect to the rotating plane. The comparison of the experiment with the prior statistical calculation suggests that the intramolecular hydrogen-bond energy of hexafluoroacetylacetone might be smaller than that of acetylacetone.

Acknowledgment. This work was financially supported by Korea Research Foundation (Project No. 1998-015-D00158) and 1999 Inha University Fund.

References and Notes

- (1) Powling, J.; Bernstein, H. J. *J. Am. Chem. Soc.* **1951**, *73*, 4553.
- (2) Nakanishi, H.; Morita, H.; Nagakura, S. *Bull. Chem. Soc. Jpn.* **1977**, *50*, 2255.
- (3) Dannenberg, J.; Rios, R. J. *Phys. Chem.* **1994**, *98*, 6714.
- (4) Lowrey, A. H.; George, C.; D'Antonio, P.; Karle, J. *J. Am. Chem. Soc.* **1971**, *93*, 6399.
- (5) Iijima, K.; Ohnogi, A.; Shibata, S. *J. Mol. Struct.* **1987**, *156*, 111.
- (6) Hush, N. S.; Livett, M. K.; Peel, J. B.; Willett, G. D. *Aust. J. Chem.* **1987**, *40*, 599.
- (7) Brown, R. S. *J. Am. Chem. Soc.* **1977**, *99*, 5497.
- (8) Isaacson, A. D.; Morokuma, K. *J. Am. Chem. Soc.* **1975**, *97*, 4453.
- (9) Choi, C.; Pintar, M. M. *J. Chem. Phys.* **1977**, *106*, 3473.
- (10) Karlström, G.; Jönsson, B.; Roos, B.; Wennerström, H. *J. Am. Chem. Soc.* **1976**, *98*, 6851.
- (11) Krokidis, X.; Goncalves, V.; Savin, A.; Silvi, B. *J. Phys. Chem. A* **1998**, *102*, 5065.
- (12) Hinsin, K.; Roux, B. *J. Chem. Phys.* **1997**, *106*, 3567.
- (13) Yoon, M.-C.; Choi, Y. S.; Kim, S. K. *Chem. Phys. Lett.* **1999**, *300*, 207.
- (14) Yoon, M.-C.; Choi, Y. S.; Kim, S. K. *J. Chem. Phys.* **1999**, *110*, 11850.
- (15) Walzl, K. N.; Xavier, I. M., Jr.; Kuppermann, A. *J. Chem. Phys.* **1987**, *86*, 6701.
- (16) Roubin, P.; Chiavassa, T.; Verlaque, P.; Pizzala, I.; Bodot, H. *Chem. Phys. Lett.* **1990**, *175*, 655.
- (17) Ogoshi, H.; Nakamoto, K. *J. Chem. Phys.* **1966**, *45*, 3113.
- (18) Kondo, K.; Kondo, Y.; Takemoto, T.; Ikegami, T. *J. Chem. Soc. Jpn.* **1965**, *68*, 1404.
- (19) Dieke, G. H.; Crosswhite, H. M. *J. Quant. Spectrosc. Radiat. Transfer* **1962**, *2*, 97.
- (20) Chidsey, I. L.; Crosley, D. R. *J. Quant. Spectrosc. Radiat. Transfer* **1980**, *23*, 187.
- (21) Hunnicutt, S. S.; Waits, L. D.; Guest, J. A. *J. Phys. Chem.* **1991**, *95*, 562.
- (22) Vasudev, R.; Zare, R. N.; Dixon, R. N. *J. Chem. Phys.* **1984**, *80*, 4863.
- (23) The molecular geometry of the enolic hexafluoroacetylacetone in the ground state has been optimized using a 6-31G(d) basis set on the HF level.
- (24) Gilbert, R. G.; Smith, S. C. *Theory of Unimolecular and Recombination Reactions*; Blackwell: Oxford, 1990.